Oscillation Energies of Colliding Raindrops

DAVID B. JOHNSON AND KENNETH V. BEARD[1]

Illinois State Water Survey, Champaign, IL 61820

(Manuscript received 2 August 1983, in final form 12 December 1983)

ABSTRACT

When raindrops collide, some of the kinetic energy involved in the collision will be available to initiate or sustain oscillations in the surviving drops. This paper presents results of a simple model of drop collisions that generates an estimate of the expected distribution of energies in an ensemble of colliding raindrops as a function of drop size and rain intensity. The results indicate that drop collisions can be an effective source of raindrop oscillations and that, within any one rain shaft, it tends to produce a range of oscillation energies from intense to imperceptible. In every case, however, the fraction of drops oscillating and the severity of the oscillations increase with increasing drop size and rainfall intensity.

1. Introduction

When two raindrops collide, they can either bounce off one another, coalesce, or break into fragments. No matter what fate awaits the colliding drops, however, some of the kinetic energy involved in the collision will manifest itself in mechanical oscillations of the drop or group of drops that survive the collision. When viewed at night with suitable illumination, this sort of oscillation is readily apparent in natural rainfall (e.g., Blanchard, 1962). While there are a variety of other energy sources that at times may be capable of driving drop oscillations (such as turbulent air motions, wake shedding, or fall into strongly sheared environments), the collisional energy source is particularly intriguing since it provides an inherent oscillation mechanism that does not require special conditions or circumstances. While it is not clear whether surface observations of raindrop oscillation such as Blanchard's are caused by collisions or by other energy sources, it is certain that collisions are an integral part of raindrop existence and whenever drops collide, oscillations will be triggered.

The degree to which a colliding raindrop stays in an agitated state, of course, will depend on the collision rate and amount of energy provided by each collision as well as the rate at which the oscillations are damped by viscosity. In a previous paper (Beard *et al.*, 1983), we examined the collisional mechanism for raindrop oscillation by means of a model which produced an estimate of the average energy levels associated with a balance between dissipation of oscillational energy and its rate of supply by collisions with other raindrops. That study concluded that collisions could provide sufficient energy to produce large-amplitude oscillations in moderate-to-heavy rainfall. Under such circumstances drop collisions are likely to be the dominant energy source for oscillations. While the energy balance model is adequate to examine the overall magnitude of the collisional energy source, it can be a bit restrictive since it generates only a single estimate of an average oscillation energy and gives no information about the fraction of drops oscillating in any particular energy range. In the present paper, we reexamine the question of collision-induced drop oscillations using a probabilistic interpretation of the coalescence equations similar to that employed in stochastic collection models to generate an estimate of the full distribution of oscillation energies as a function of drop diameter and rainfall rate. The depiction of the results in terms of the distribution of energies in an ensemble of colliding raindrops is a significant extension of our earlier work giving a more realistic physical picture of collision-induced oscillations.

2. Model formulation

The goal of this model is to calculate the oscillation energies of large raindrops resulting from collisions with smaller drops. The model starts with the same basic assumptions as were invoked in Beard *et al.* (1983), but extends the calculations to produce estimates of the full distribution of oscillation energies. Computations are performed for each of a number of different raindrop distributions. Each distribution is assumed to be at least quasi-steady state, so any changes in the distribution resulting from coalescence or breakup can be ignored. To describe adequately the raindrop distribution, 112 logarithmically-spaced drop categories were used to cover the diameter range from

[1] Also affiliated with the Department of Atmospheric Sciences, University of Illinois.

30 μm to 5 mm with the number of drops in each class assigned as a function of rainfall rate using the equations of Sekhon and Srivastava (1971). The overall approach is based on the average collision rates between a large drop of diameter D and each smaller raindrop category, the collisional energy associated with each collision, and the expected rate at which the collision-induced oscillations are dissipated by viscosity in the liquid drop. The final product of each calculation is a distribution showing the fraction of large drops of diameter D having oscillation energies in any specified range.

The average number of collisions that a drop of diameter D experiences in a time step Δt with smaller drops of diameter d_i is given by

$$C_i(D, d_i) = \frac{\pi}{4}(D + d_i)^2[v(D) - v(d_i)]n(d_i)\Delta t, \quad (1)$$

where $v(D)$ and $v(d_i)$ are the terminal velocities of the drops and $n(d_i)$ is the concentration of the smaller drops. If

$$\sum_i C_i(D, d_i) \ll 1, \quad (2)$$

then an individual collision rate $C_i(D, d_i)$ can be directly interpreted as the probability that the large drop will undergo a collision with a drop of diameter d_i in the time interval Δt.

As discussed in Beard *et al.* (1983), the excess kinetic energy associated with a collision between a large drop of diameter D and a smaller drop of diameter d_i can be expressed as

$$E_{ki}(D, d_i) = \tfrac{1}{2}Mv(D)^2 + \tfrac{1}{2}mv(d_i)^2 - \tfrac{1}{2}[Mv(D) + mv(d_i)]^2/(M + m), \quad (3)$$

where M and m are the masses of the drops of diameters D and d_i, respectively and, as before $v(D)$ and $v(d_i)$ are their terminal velocities. This estimate of the excess energy ignores the possible energy contribution of a reduction in surface area associated with coalescence and is equivalent to the collisional kinetic energy discussed by McTaggart-Cowan and List (1975).

For drop oscillation (or drop breakup) studies, it is useful to nondimensionalize the energy terms by use of the surface energy of the drop, $E_s(D)$, such that

$$\mathscr{E}_{ki} \equiv E_{ki}(D, d_i)/E_s(D),$$

$$\mathscr{E} \equiv E(D)/E_s(D),$$

where $E(D)$ is the oscillation energy of a drop of diameter D, and E_{ki} is the excess kinetic energy defined by (3). This same nondimensionalization will be used throughout this study; it is identified by use of a script $\mathscr{E}$.

The dissipation of energy by a vibrating drop of diameter D can be estimated by the relation

$$\frac{d\mathscr{E}}{dt} = \frac{-2\mathscr{E}}{\tau}, \quad (4)$$

where τ, the time constant of amplitude decay for the fundamental mode, is given by

$$\tau = D^2/(20\nu),$$

and ν is the kinematic viscosity of liquid water. Since the energy decays exponentially, it is convenient to introduce discrete energy categories, $\mathscr{E}_j$, that are spaced logarithmically. In this case, the time step Δt can be selected so that the energy dissipation during one time step always reduces the energy by a single category. For example, if the energy categories are spaced by $\Delta \log\mathscr{E}_j = \epsilon$, then the desired time step is $\Delta t = 2.303\epsilon\tau/2$. In the present model, 55 logarithmically spaced energy categories are use to describe the nondimensionalized oscillation energies from 0.001 to 0.5 ($\epsilon = 0.05$). With the use of this value of ϵ the appropriate time step Δt becomes 0.05756τ. Fortunately, this time step is short enough that the inequality (2) is satisfied for all cases with $D < 5$ mm and rainfall rates < 100 mm h^{-1}. The upper limit on the energy classifications ($\mathscr{E} = 0.5$) is assumed to correspond to the maximum oscillation that can be supported by a raindrop without breakup (Beard *et al.*, 1983; List *et al.*, 1980). The lower energy limit ($\mathscr{E} = 0.001$) represents an estimate of the smallest oscillation energies that are likely to produce significant deviations from equilibrium shapes. This estimate is based on potential energy "well" calculations such as shown in Fig. 3 in Beard *et al.* (1983). An additional energy category ($\mathscr{E} = 0$) is used to keep track of all drops that are not yet oscillating or whose oscillations have decayed below the $\mathscr{E} = 0.001$ energy level.

A separate calculation is performed for each raindrop distribution (specified by its rainfall rate) and for each large drop diameter D. The fundamental parameter to be followed is N_j, the number of raindrops of diameter D having oscillation energies in category $\mathscr{E}_j$. If the probability of a drop D striking a smaller drop d_i during a time step Δt is C_i and the collisional kinetic energy associated with that collision is $\mathscr{E}_{ki}$, then N_jC_i drops are transferred from the $\mathscr{E}_j$ category to a new energy category $\mathscr{E}_m$ that corresponds to an energy level of $\mathscr{E} = \mathscr{E}_j + \mathscr{E}_{ki}$ while $(1 - C_i)N_j$ drops remain in the category $\mathscr{E}_j$. If $\mathscr{E}_j + \mathscr{E}_{ki} > 0.5$, then breakup is invoked with the assumption that each of these collisions produces one large fragment, corresponding to the initial large drop, that survives the breakup and carries away the maximum oscillation energy permitted ($\mathscr{E} = 0.5$). Excess energy beyond $\mathscr{E} = 0.5$ is ignored, as are the other fragments produced during breakup. While there are little or no data available on the partitioning of the oscillation energy during drop breakup, the assumption that a large fragment corresponding to the initial large drop is created in most breakup events is generally supported by observational studies (List *et al.*, 1980). After redistribution of the drops in each of the 56 energy categories for every possible collision

such that $d_i < D$, time is incremented and all drops decay to the next lower energy level.

Initially, all drops are assigned to the $\mathcal{E} = 0$ (non-oscillating) category. Once the computations begin, however, all possible energy states become occupied as the average energy increases and the distribution converges toward steady state. Fig. 1 shows one aspect of the evolution of the model. This example illustrates the buildup of the mean oscillation energy of 4 mm drops for five different droplet distributions. After a rapid initial rise, the mean energy quickly levels off at, or slightly below, the level predicted by the steady-state energy balance model of Beard *et al.* (1983). The difference between the steady-state mean energies predicted by the current model and those predicted by the energy balance model are solely due to different breakup criteria used in each. In the energy distribution model, any drop whose total energy following collision exceeds $\mathcal{E} = 0.5$ is assumed to break up. In the energy balance model, on the other hand, breakup was invoked only when the kinetic energy associated with any one collision exceeded $\mathcal{E}_{ki} = 0.5$. If the mean energy levels are low, there is very little difference between these criteria. As the mean energies increase, however, the difference between the models also increases, with the energy distribution model predicting lower mean energies. Fig. 2 shows the steady-state mean energies predicted by the energy distribution model as a function of drop diameter and rainfall rate. These mean energies, as well as the energy distributions discussed in the next section, were obtained after a time interval of 8τ from the start of the computations, in order to ensure that model predictions reflect steady-state conditions.

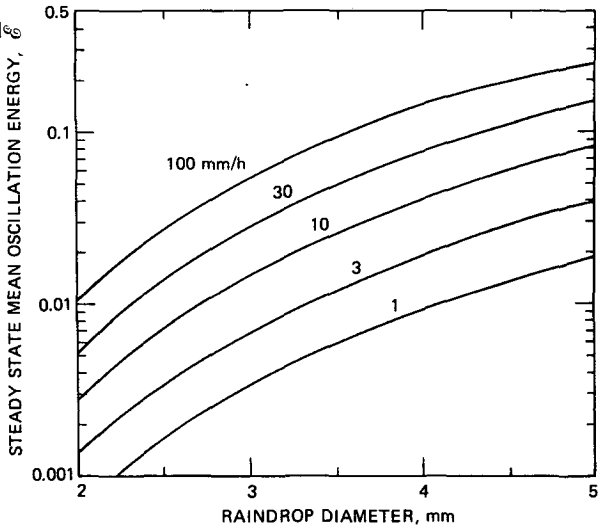

FIG. 2. Steady-state mean oscillation energies from the energy distribution model as a function of drop size and rainfall rate.

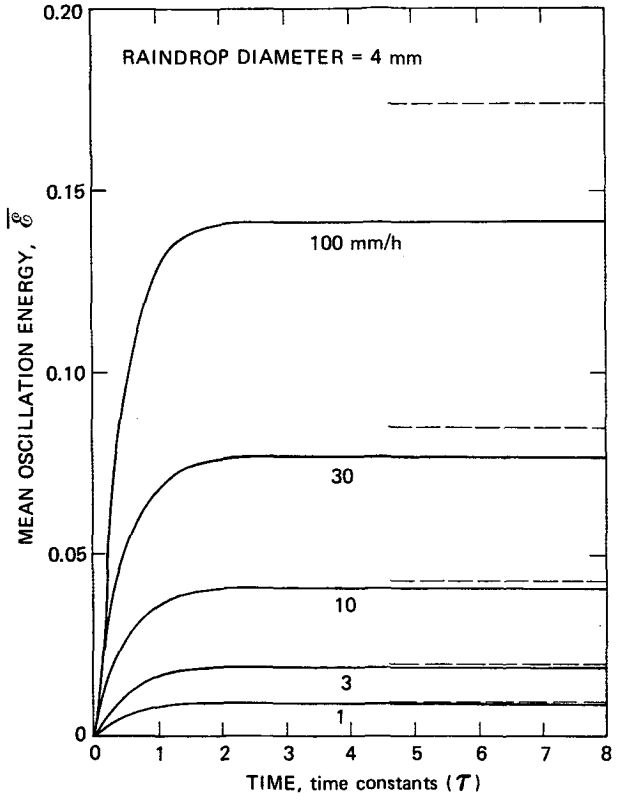

FIG. 1. Time evolution of the nondimensionalized mean oscillation energy for five different ensembles of 4 mm diameter raindrops in terms of the time constant for amplitude decay for the fundamental mode. Each curve corresponds to a different raindrop distribution and is labeled in terms of the overall rainfall rate of the distribution. The thin dashed horizontal lines represent corresponding estimates of the mean energies from the steady-state energy balance model of Beard *et al.* (1983).

3. Model results

Figures 3–8 illustrate the steady-state number density distributions of raindrops with diameters ranging from 2.5 to 5.0 mm as a function of the nondimensionalized oscillation energies ($\mathcal{E}$). Within each figure, separate distributions are shown for rainfall rates up to 100 mm h^{-1}. In this type of presentation, the area under each curve is proportional to the total fraction of drops oscillating within the range of energies plotted. The increase in area beneath the curves for higher rainfall rates and larger drop diameters merely reflects a larger fraction of drops having oscillation energies between $\mathcal{E} = 0.001$ and $\mathcal{E} = 0.5$. For convenience, Tables 1–3 provide an alternative view of the same results. Table 1 shows the fraction of drops having oscillation energies greater than a tenth of 1% of their surface energies as a function of raindrop diameter and rainfall rate. Tables 2 and 3 show similar data for drops oscillating with energies greater than 1% and 10% of their surface energies, respectively.

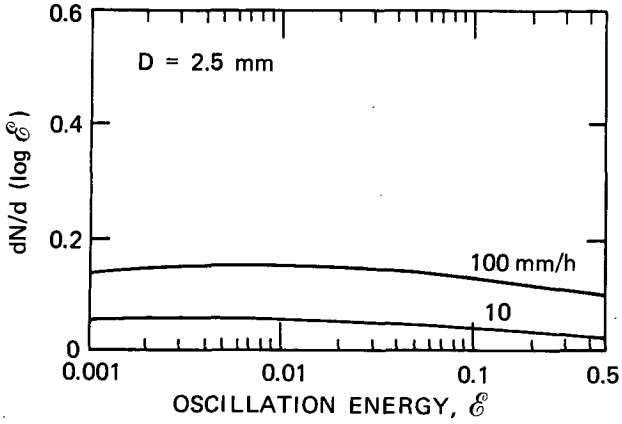

FIG. 3. Steady-state number density distributions for 2.5 mm diameter raindrops as a function of the nondimensionalized oscillation energy. Separate curves are shown for rainfall rates of 10 and 100 mm h^{-1}.

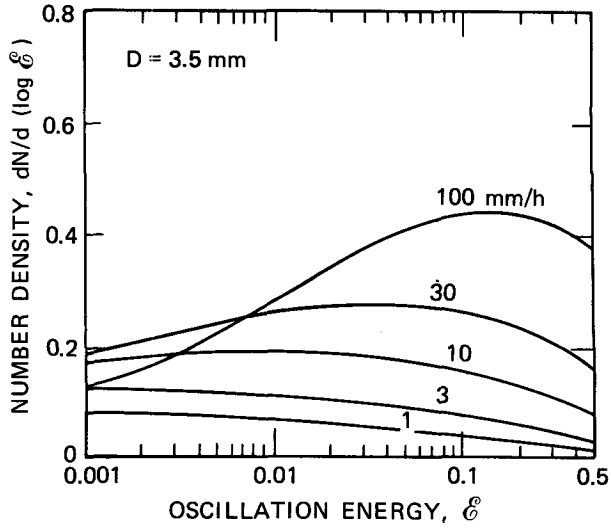

FIG. 5. As in Fig. 3, but for 3.5 mm diameter raindrops. Separate curves are shown for five different rainfall rates.

Taken collectively these results indicate that at any instant, a suitable ensemble of colliding raindrops will contain drops having oscillation energies that range from intense to imperceptible. At the level of the individual drops, this distribution of energies is understandable since the collisional mechanism for generating oscillations is inherently unsteady with irregularly repeated cycles of sudden energy input followed by gradual decay. If drops with oscillation energies smaller than $\mathcal{E} = 0.001$ are classified as not oscillating, there is almost always a significant number of nonoscillating drops. This remains the case even when the mean oscillation energies are quite high. In every case, however, both the fraction of drops oscillating and the severity of the oscillations increase as the drop diameter and rainfall rate increase. For example, the model suggests that 86% of the 3 mm diameter raindrops in a 3 mm h^{-1} rainshaft would be expected to have oscillation energies less than $\mathcal{E} = 0.001$ (not oscillating), while only 2% are oscillating intensely with $\mathcal{E} > 0.1$. With an increase in the rainfall rate to 30 mm h^{-1}, 58% of the drops are not oscillating, while 9% are oscillating intensely. On the other hand, if we consider drops as large as 5 mm, then the model predicts that 32% of these drops will not be oscillating in a 3 mm h^{-1} rainfall and 13% will have oscillations with $\mathcal{E} > 0.1$. With a 30 mm h^{-1} rain rate, only 1% of the 5 mm raindrops would not exhibit appreciable oscillations while 53% would exhibit strong oscillations.

In an interpretation of these results it is important to explore which collisions contribute the most energy to drop oscillations. Using the current nomenclature,

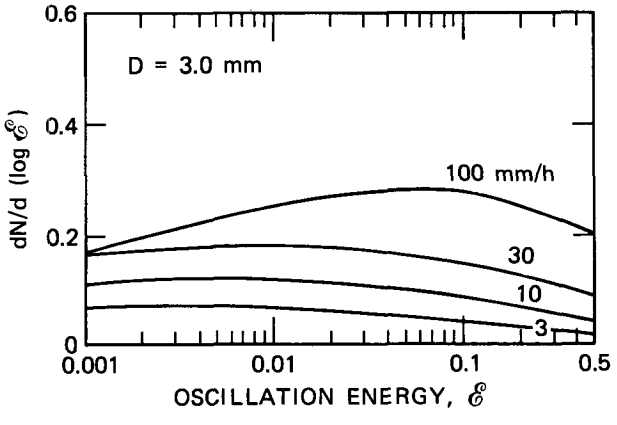

FIG. 4. As in Fig. 3, but for 3.0 mm diameter raindrops. Separate curves are shown for four different rainfall rates.

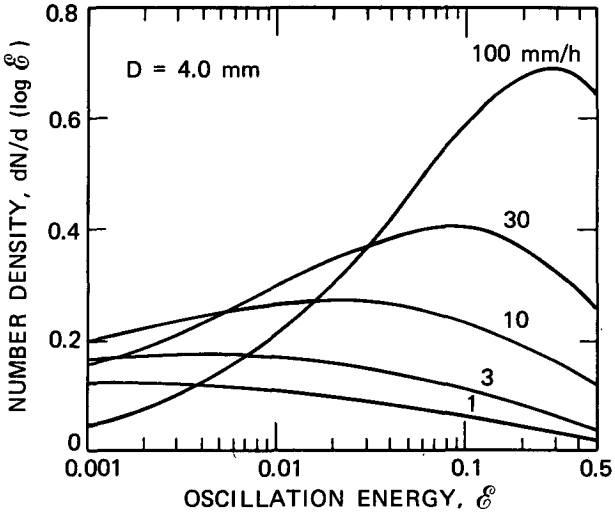

FIG. 6. As in Fig. 3, but for 4.0 mm diameter raindrops. Separate curves are shown for five different rainfall rates.

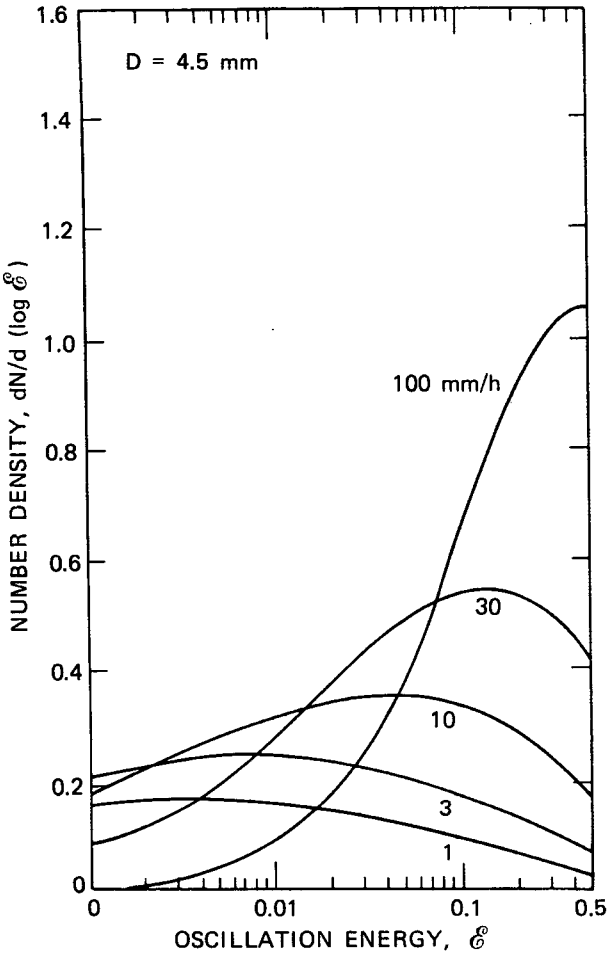

FIG. 7. As in Fig. 3, but for 4.5 mm diameter raindrops. Separate curves are shown for five different rainfall rates.

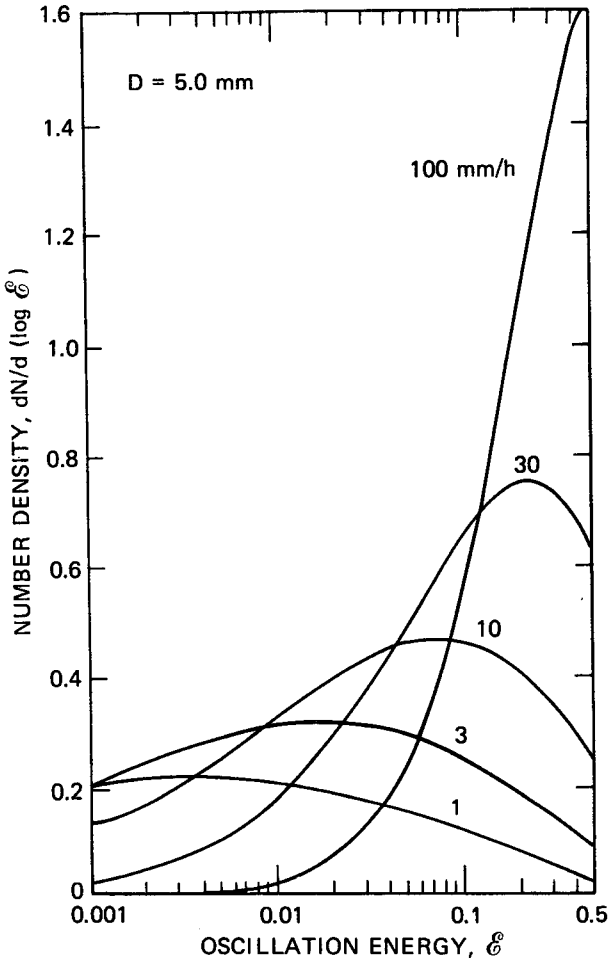

FIG. 8. As in Fig. 3, but for 5.0 mm diameter raindrops. Separate curves are shown for five different rainfall rates.

we note that the overall rate at which collisional energy is supplied to a raindrop of diameter D can be expressed as $\dot{\mathcal{E}}_k = \Sigma\, \mathcal{E}_{ki} C_i / \Delta t$. Fig. 9 shows the density distribution functions for $\dot{\mathcal{E}}_k$ as a function of the small drop diameter d_i for five different rainfall rates. In this case, the area under each curve is proportional to the total rate of collisional energy input. Similarly, the contribution toward the total energy input from collisions with any specified size-range of smaller raindrops is proportional to the area under that portion of the curve. In order to limit the energy contribution from collisions resulting in breakup, Fig. 9 has been constructed with the limitation that the maximum energy supplied by any one collision is $\mathcal{E}_{ki} = 0.5$. This limit is identical to the constraint employed in our earlier energy balance model. To the left of the peak, collisions result in coalescence, while to the right, collisions result in breakup. Since all collisions that result in breakup are assumed to supply the same energy, the reduction in energy contributions to the right of the peak merely reflects the drop-off in the frequency of collisions. To the left of the peak, the energy in each collision drops off rather sharply, while the collision rate levels off and begins to decline as well. In the example shown (D = 4 mm), most of the oscillation energy is supplied by collisions with drops in the size interval from 300 μm to 2 mm diameter with the peak contributions between 500 and 600 μm diameter.

TABLE 1. Fraction of raindrops having oscillation energies $\mathcal{E}$ greater than 0.1% of their surface energies.

Rainfall rate (mm h^{-1})	Raindrop diameter (mm)						
	2.0	2.5	3.0	3.5	4.0	4.5	5.0
1	0.014	0.037	0.077	0.138	0.222	0.327	0.445
3	0.027	0.068	0.140	0.245	0.380	0.533	0.683
10	0.051	0.129	0.257	0.430	0.619	0.789	0.908
30	0.090	0.223	0.422	0.649	0.839	0.950	0.991
100	0.163	0.383	0.655	0.873	0.975	0.998	1.000

TABLE 2. Fraction of raindrops having oscillation energies $\mathcal{E}$ greater than 1% of their surface energies.

Rainfall rate (mm h^{-1})	Raindrop diameter (mm)						
	2.0	2.5	3.0	3.5	4.0	4.5	5.0
1	0.007	0.019	0.038	0.069	0.111	0.167	0.233
3	0.014	0.036	0.074	0.132	0.209	0.309	0.422
10	0.028	0.071	0.145	0.254	0.391	0.547	0.700
30	0.051	0.129	0.257	0.430	0.622	0.795	0.916
100	0.095	0.236	0.446	0.682	0.869	0.967	0.996

To the extent that the areas on each side of the peak in curves like those shown in Fig. 9 are equal, then collisions resulting in coalescence and breakup should contribute equally to the forcing of oscillations. In explaining the overall shape of the energy distributions (Figs. 3–8), however, we note that the critical parameter seems to be the time interval between collisions, and in particular the interval between the more energetic collisions. If these collisions are relatively infrequent, there is enough time for the oscillations produced to decay most or all of the way across the energy domain. When the energy scale is presented logarithmically, as in the present case, this tends to result in a flat distribution. If energetic collisions are frequent, then there will be a buildup of drops in the upper end of the energy distribution. As the average energy increases, it becomes increasingly likely that each new collision may be able to add enough energy to the oscillating drop to cause it to break up. This tends to create a gradual shift in importance from coalescence events to breakup events as energy levels increase.

4. Discussion

This study reinforces our earlier conclusion that drop collisions can be an important energy source for drop oscillations (Beard *et al.*, 1983), while emphasizing that there will always be a wide range of intensities of oscillation in any ensemble of drops undergoing collisional excitation. Although other energy sources may also contribute to oscillations in special situations, the collisional energy source would seem to have widespread applicability since it will always be present when drops exist in sufficient numbers to collide with one another. Although it may be possible to find an example of almost any level of oscillation within a single rainshaft, ranging from drops oscillating at the verge of breakup to those with motions that are so thoroughly damped that they seem to be at rest, the number of drops oscillating and the intensity of the oscillations will always increase with increasing drop size and rainfall rate.

TABLE 3. Fraction of raindrops having oscillation energies $\mathcal{E}$ greater than 10% of their surface energies.

Rainfall rate (mm h^{-1})	Raindrop diameter (mm)						
	2.0	2.5	3.0	3.5	4.0	4.5	5.0
1	0.002	0.005	0.010	0.018	0.028	0.043	0.057
3	0.004	0.011	0.022	0.039	0.061	0.092	0.127
10	0.009	0.023	0.046	0.084	0.134	0.202	0.284
30	0.017	0.044	0.091	0.164	0.260	0.385	0.527
100	0.033	0.088	0.180	0.318	0.490	0.675	0.835

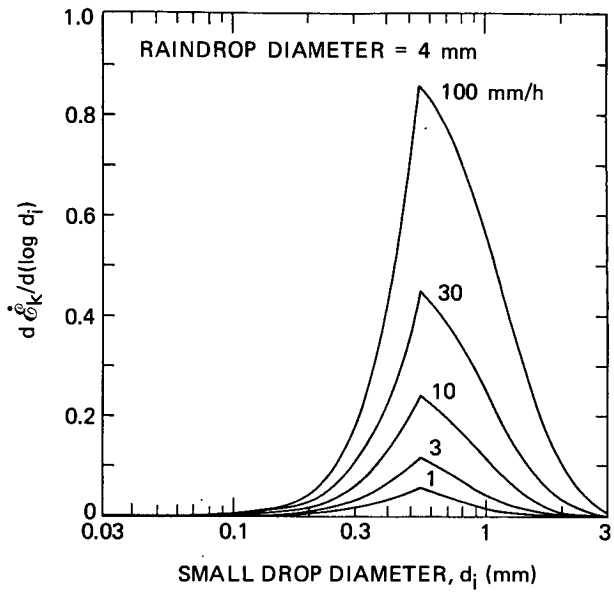

FIG. 9. Density distribution functions for $\dot{\mathcal{E}}_k$, the rate of collisional energy input, for a 4 mm diameter raindrop as a function of the small drop diameter d_i. Separate curves are shown for five different rainfall rates.

While these results should be useful in understanding some of the general features of the collisional forcing of raindrop oscillations, the specific numbers produced by the model should be taken with some caution. The model includes only one energy source and is by no means a complete description of that one. For example, the smaller fragments resulting from breakup and their oscillations are not considered by the model. Furthermore, it should be noted that there will be situations in which the model predictions may significantly overestimate or underestimate the intensity of the oscillations. Fig. 9, for example, reveals the sensitivity of the model results to the small end of the raindrop distribution, and any process that modifies the relative concentration of these drops will have a direct impact in the intensity of the collisional forcing (e.g., List *et al.*, 1980). Size-sorting of particles within a precipitation shaft is one example of a process that will clearly impact on the collisional forcing. In addition, any residual fragments of unmelted ice (or even air bubbles left in the process of melting) may be expected to enhance

the speed with which oscillations are damped (Blanchard, 1950, 1957) and may produce significant shifts in the expected energy distributions. Similarly, the introduction of oscillation energy in modes higher than the fundamental is likely to speed damping and shift the energy distributions toward lower energies.

In this analysis, we have concentrated exclusively on the oscillation energies and not on the shapes of the oscillating drops. While it is possible to translate the current results into drop-shape distributions (e.g., Beard and Johnson, 1984), such an extension is somewhat speculative. It is not clear, for example, that this approach will be adequate for large amplitude oscillations. More importantly, this approach assumes a detailed knowledge of the mode or modes of oscillation expected for a particular situation and, at present, our knowledge of these modes is rather limited.

Acknowledgments. This work was supported by the National Science Foundation under Grants ATM81-08455 and ATM82-16847. Discussions with Dr. Arthur Jameson of the Illinois State Water Survey were instrumental in the development of this approach.

REFERENCES

Beard, K. V., and D. B. Johnson, 1984: Raindrop axial and backscatter ratios using a collisional probability model. *Geophys. Res. Lett.*, **11,** 65–68.

——, —— and A. R. Jameson, 1983: Collisional forcing of raindrop oscillations. *J. Atmos. Sci.*, **40,** 455–462.

Blanchard, D. C., 1950: The behavior of water drops at terminal velocity in air. *Trans. Amer. Geophys. Union,* **31,** 836–842.

——, 1957: The supercooling, freezing, and melting of giant waterdrops at terminal velocity in air. *Artificial Stimulation of Rain,* Pergamon Press, 233–249.

——, 1962: Comments on the breakup of raindrops. *J. Atmos. Sci.*, **19,** 119–120.

List, R., T. B. Low, N. Donaldson and E. Freire, 1980: Experiments and models on coalescence and breakup of raindrops. *Proc. Int. Conf. Cloud Physics,* France, 165–168. [Available from WMO, Geneva.]

McTaggart-Cowan, J. D., and R. List, 1975: Collision and breakup of water drops at terminal velocity. *J. Appl. Meteor.*, **32,** 1401–1411.

Sekhon, R. S., and R. C. Srivastava, 1971: Doppler radar observations of drop-size distributions in a thunderstorm. *J. Atmos. Sci.*, **28,** 983–994.